Application of a Functional 3-dimensional Perfusion Model in Laparoscopic Partial Nephrectomy With Precise Segmental Renal Artery Clamping

Shaobo Zhang, Guanyu Yang, Lijun Tang, Qiang Lv, Jie Li, Yi Xu, Xiaomei Zhu, Pu Li, Pengfei Shao, and Zengjun Wang

OBJECTIVES To assess the feasibility of a novel functional perfusion model based on enhanced computed tomography (CT) for the evaluation of split renal function and orientation of segmental renal artery clamping during laparoscopic partial nephrectomy (LPN).

MATERIALS AND METHODS From December 2016 to November 2017, functional perfusion model was applied in 91 patients with T1a renal tumors who had undergone LPN with segmental renal artery clamping. Split computed tomographic-glomerular filtration rate (CT-GFR) was calculated using the 2-point Patlak plot technique. Parenchymal perfusion areas of segmental renal arteries were marked, and target segmental arteries were determined by the perfusion areas wherein tumors were confined. LPN with precise segmental renal artery clamping was performed based on the novel model. Correlations between CT-GFR and estimated GFR and radioisotope GFR were analyzed using Pearson's method. Intraoperative ischemic status and surgical outcomes were assessed.

RESULTS Mean tumor size was 2.9 cm. Large tumors were accompanied by more feeding lobar arteries than segmental arteries. CT-GFR was strongly correlated with estimated GFR ($r = 0.70$) and radioisotope GFR ($r = 0.88$). All LPNs were successful without converting to main renal artery clamping. Mean operation time was 81.8 minutes; median estimated blood loss was 120 mL. The actual parenchymal ischemic region observed during the operation was consistent with the prediction of the perfusion model in all patients. No arterial bleeding or other uncontrollable defect bleeding occurred during tumor resection.

CONCLUSION This model is a reliable method for the determination of split renal function and orientation of segmental artery clamping during LPN. UROLOGY 125: 98–103, 2018. © 2018 Elsevier Inc.

Laparoscopic partial nephrectomy (LPN) is widely accepted as a minimally invasive nephron-sparing surgery for T1a renal tumors.[1,2] Precise segmental artery clamping is safe and feasible, preventing global renal ischemia.[3-5] In our previous studies, computed tomography angiography (CTA) revealed the arterial vasculature within the hilum.[5,6] The target arteries were determined if arterial branches were directly entering or abutting the tumor.[6,7] However, CTA is unable to depict the actual perfusion of the parenchyma by different segmental arteries. This may lead to insufficient clamping, with arterial bleeding or excessive ischemia occurring in patients. Novel models providing precise information regarding target segmental arteries according to the parenchymal perfusion areas of different segmental arteries are required.

LPN with precise segmental artery clamping has the advantage of protecting postoperative renal function. The glomerular filtration rate (GFR) is usually evaluated by radionuclide renography. However, this increases medical costs and is linked to potential radiation risk. Therefore, an alternative method to evaluate GFR is warranted for nephron-sparing surgery. Previous studies have shown

Funding Support: This research was supported by Key Research and Development Project of Jiangsu Province (BE2018749), National Natural Science Foundation under grants (31571001), Science Foundation for The Excellent Youth Scholars of Southeast University.

From the Department of Urology, The First Affiliated Hospital of Nanjing Medical University, Nanjing, China; the Key Laboratory of Computer Network and Information Integration, Southeast University, Ministry of Education, Nanjing, China; and the Department of Radiology, The First Affiliated Hospital of Nanjing Medical University, Nanjing, China

Address correspondence to: Pengfei Shao, M.D., Ph.D., Department of Urology, The First Affiliated Hospital of Nanjing Medical University, 300 Guangzhou Road, Nanjing 210029, China. E-mail: spf8629@163.com

Submitted: October 23, 2018, accepted (with revisions): December 17, 2018

https://doi.org/10.1016/j.urology.2018.12.023
0090-4295

that the evaluation of GFR using contrast-enhanced computed tomography (CT) is feasible in cases with renal transplantation and renal artery stenosis.[8,9]

In this study, we integrated a novel functional 3-dimensional (3D) perfusion model using a single CT examination to meet the requirement of renal function evaluation and parenchymal perfusion divided by segmental arteries. Moreover, we assessed the feasibility of this integrated 3D perfusion model in patients undergoing LPN with segmental renal artery clamping.

PATIENTS AND METHODS

Patients ($n = 91$) underwent LPN with precise segmental clamping from December 2016 to November 2017. Eligible patients signed a written informed consent form approved by the institutional review board. Inclusion criteria were (1) a single localized mass ≤4 cm (T1a); (2) normal contralateral kidney; and (3) normal levels of serum creatinine (SCr) prior to the operation. All the patients underwent routine testing and dual-source CT (DSCT). RENAL nephrometry scores were collected.[10] According to CT, presence of an endophytic, mesophytic, and exophytic tumor was considered when <40%, 40%-60%, and >60% of the mass was protruding, respectively.[11]

GFR Measurement

In the first 15 patients, split GFRs of bilateral kidneys were measured as radioisotope GFR (Ri-GFR) through radionuclide renography using technetium $^{99\ m}$Tc diethylenetriaminepentaacetic acid (Gate's method). SCr was determined in all the 91 patients, and eGFR was calculated according to the Chronic Kidney Disease Epidemiology Collaboration equation[12] ($eGFR = a*[SCr/b]^{c}*[0.993]^{age}$). For males, $a = 141$, $b = 0.9$, or $c = -0.411$ ($SCr \leq 79.6$ μmol/L) or $c = -1.209$ ($SCr > 79.6$ μmol/L). For females, $a = 144$, $b = 0.7$, or $c = -0.329$ ($SCr \leq 61.9$ μmol/L) or $c = -1.209$ ($SCr > 61.9$ μmol/L).

During DSCT, patients were injected with nonionic contrast media (iopromide, 370 mg I/mL) and scanned in the early parenchyma phase. According to the Patlak equation,[13] 2-point Patlak plot technique[14] was used to describe the 2-compartment model, referring to renal vessels and tubules. The amount of contrast media in the entire kidney K(t) was expressed as the sum of contrast media in the vascular space B(t) and nephron N(t). It was assumed that the amount of contrast media in the vascular space B(t) was proportional to that in the aorta, whereas the amount of contrast media filtered into the nephron was proportional to the integral of concentration of contrast media in the aorta (Supplementary Fig. 1). Thus, a customized GFR quantitative software was developed. The data from kidney DSCT scans were analyzed using the software, and split (s)CT-GFR in the presence or absence of a kidney tumor was calculated. The combined values of sCT-GFR formed the total (t)CT-GFR, standardized by body surface area.

Segmental Perfusion Image

Anatomically, the renal artery splits into several segmental arteries, further dividing into lobar arteries within the renal sinus or parenchyma. Different lobar arteries supply different parenchymal regions. The supply boundary of the adjacent 2 lobar arteries is the midline of these 2 arteries (Supplementary Fig. 2). In the integrated 3D perfusion model, lobar arteries were vertically projected to the parenchyma (black dotted line) and the boundary of the perfusion areas was middle of projection of adjacent 2 lobar arteries (yellow dotted line). Using the semimanual depiction method based on the platform of MeVisLab 2.1 (https://www.mevislab.de), we depicted the perfusion boundary of every 2 adjacent lobar arteries. According to the relationship of lobar arteries and segmental arteries, the perfusion areas of lobar arteries were jointed together, and then the renal segmental arteries and their perfusion areas in the parenchyma were marked with different colors (Figs. 1, 2). Subsequently, target segmental arteries were determined by the perfusion areas wherein the renal tumor was confined (Figs. 1, 2).

Surgical Technique

As described previously,[6] patients were anesthetized (general) and placed in the lateral decubitus position. Four trocars were applied. The renal hilum was approached through the anterior or posterior pathway according to the orientation of the target segmental arteries shown in the model. Subsequently, 1-3 target segmental arteries were isolated and clamped using a bulldog clamp. After target artery clamping, the boundary of the ischemic region was recorded (Figs. 1, 2). The tumor was resected with approximately 0.5 cm to the tumor capsule. Subsequently, the tumor bed and parenchymal defect were sutured using 2-0 barb sutures. Finally, the bulldog clamp was removed, and the specimen was retrieved.

Statistical Analysis

Postoperative complications were analyzed according to the Clavien-Dindo system.[15] Complication data were collected based on Martin's criteria.[16] Student's t test was used to assess the correlation between tumor size and the number of arteries. The 2-sided χ^2 test was performed to assess the correlation between the growth pattern and number of arteries. The correlation between tCT-GFR and eGFR or Ri-GFR was evaluated through Pearson's correlation coefficients using SPSS 23.0 software. Strong correlation was defined as correlation coefficients (r) > 0.6. A P value < 0.05 was considered statistically significant.

RESULTS

Patient Characteristics

Basic patient information is shown in Table 1. The patient population included 58 males and 33 females, aged 56.5 ± 13.6 years (range: 24-83 years), with a mean body mass index of 25.1 kg/m^2. The mean tumor size was 2.9 cm. The median RENAL nephrometry score was 5. Growth pattern results showed that exophytic, mesophytic, and endophytic tumors occupied 44.0%, 39.6%, and 16.4%, respectively. Prior to surgery, the mean eGFR was 96.5 mL min^{-1} 1.73 m^{-2}. The mean total and affected-side radioisotope GFR were 104.4 and 52.0 mL min^{-1} 1.73 m^{-2}, respectively (Supplementary Table 1).

CT-GFR and Its Correlation With eGFR and Ri-GFR

The values of sCT-GFR were calculated in the early parenchyma phase, in the presence or absence of renal tumors (Supplementary Table 1). The ratio of split CT-GFR (affected side) to total CT-GFR showed strong correlation with that of Ri-GFR ($R = 0.88$, $P < 0.01$) in 15 patients. The total CT-GFR was the sum of 2 split CT-GFRs and was compared with the eGFR in all 91 patients. The values of CT-GFR in the absence of a renal

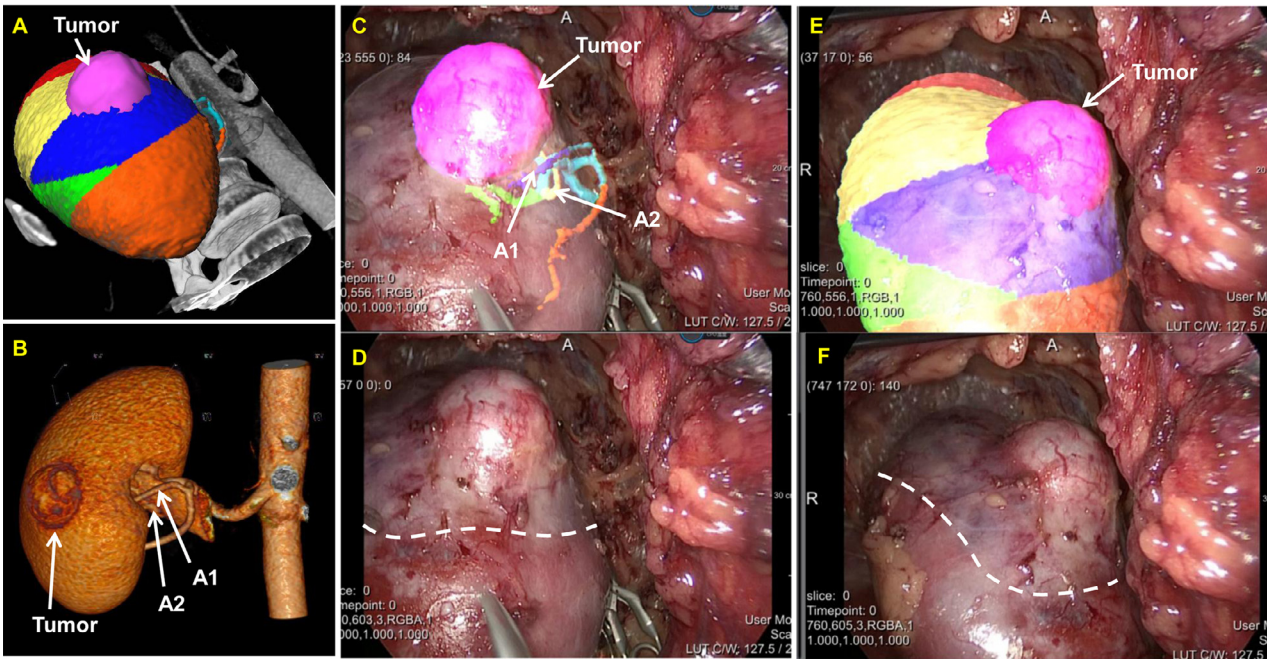

Figure 1. The application of 3D perfusion model in a patient with a 2.8 cm mesophytic tumor at the anterior side of the right kidney. (**A**) The renal parenchyma perfusion areas by different segmental arteries. The tumor was confined to yellow and blue areas. (**B**) Two target segmental arteries (A1, A2) were determined according to the perfusion areas where tumor was confined. (**C, D, E, F**) Ischemia area was demarcated after target segmental arteries were clamped during the operation. White dotted line showed the boundary of ischemia area, which was consistent with the prediction of perfusion model (Color version available online.).

tumor showed stronger correlation with eGFR compared with the values of CT-GFR in the presence of a renal tumor ($r = 0.70$, $P < 0.01$ vs $r = 0.68$, $P < 0.01$).

Data From the 3D Perfusion Model

There were 15, 41, and 35 patients with tumors supplied by 1, 2. and 3 or more feeding lobar arteries (Table 1). The corresponding mean tumor sizes were 2.1, 2.8, and 3.8 cm, respectively (Table 2). Moreover, tumors supplied by 1, 2, and 3 target segmental arteries were present in 56, 32, and 3 patients, respectively. The mean sizes of tumors supplied by 1 and 2 or more target segmental arteries were 2.9 and 3.0 cm, respectively (Table 2). A large tumor size was accompanied by more feeding lobar arteries, whereas the number of target segmental arteries showed no correlation with tumor size (Table 2). In addition, the growth pattern did not correlate with the number of arteries (regardless of the type of arteries).

Surgical Outcomes

LPN with precise segmental artery clamping orientated according to the perfusion model was successfully performed in all patients. There were no patients converted to open surgery and none required main renal artery clamping or radical nephrectomy. Following the clamping of the target arteries, the boundary of ischemia area through laparoscopy was consistent with that demonstrated in the perfusion model (Figs. 1, 2). The mean target clamping and total operation times were 19.6 and 81.8 minutes, respectively. There was no occurrence of arterial bleeding or uncontrollable hemorrhage from the tumor bed during resection. The median estimated blood loss was 120 mL (range: 50-400 mL). Postoperatively, the total complication rate was 4.4% according to the Clavien-Dindo system, including 3 patients with grade 1 complications (hematuria not requiring intervention) and 1 patient with a grade 3a complication (bleeding requiring intervention: selective embolization). The median postoperative length of stay was 6 days.

Pathologic results revealed clear-cell renal cell carcinoma ($n = 76$, 83.5%), perivascular epithelioid cell tumors ($n = 5$, 5.5%), papillary renal cell carcinoma ($n = 4$, 4.4%), chromophobe renal cell carcinoma ($n = 3$, 3.3%), oxyphilic adenoma ($n = 2$, 2.2%), and leiomyoma ($n = 1$, 1.1%). There was no positive surgical margin in all patients.

DISCUSSION

LPN with renal artery clamping is performed for the treatment of T1a renal tumors. Warm ischemia time (WIT) during operation is an independent influencing factor of renal function.[17] Warm ischemia injury may lead to histologic changes in proximal tubules when WIT was longer than 20 minutes.[18] This limitation results in technical challenges in LPN. Segmental artery clamping is a promising method for the protection of residual renal function by converting global parenchymal ischemia to regional ischemia. Driven by the variability of the renal vasculature and complexity of the renal hilum, a 3D CTA model based on DSCT was developed to recognize arteries supplying tumors. Previous studies have shown that segmental artery

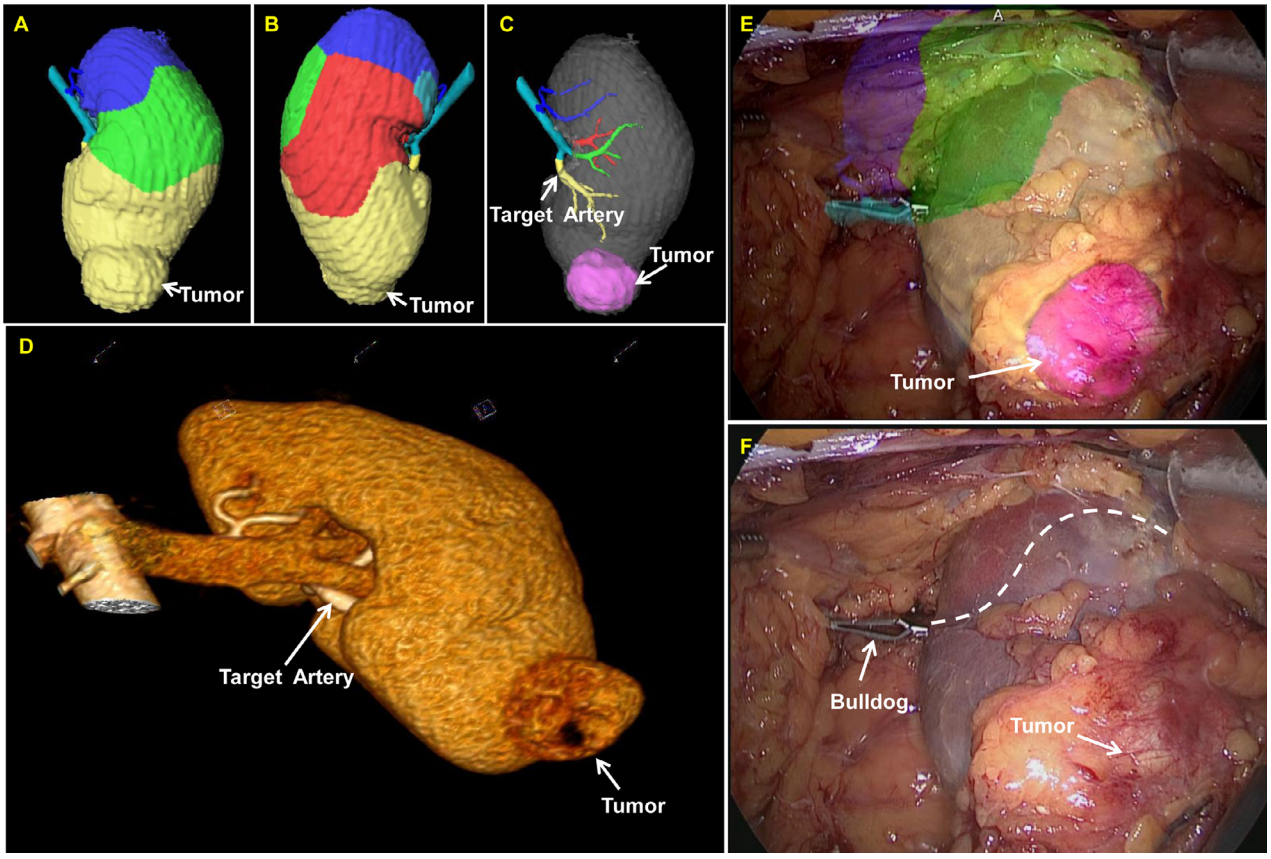

Figure 2. The application of 3D perfusion model in a patient with a 2.5 cm exophytic tumor in lower pole of the left kidney. (**A, B**) The renal parenchyma perfusion areas by different segmental arteries from anterior and posterior side. The tumor was confined to yellow areas. (**C, D**) One target segmental arteries were determined according to the perfusion areas where tumor was confined. (**E, F**) Ischemia area was demarcated after target segmental arteries were clamped during the operation. White dotted line showed the boundary of ischemia area, which was consistent with the prediction of perfusion model (Color version available online.).

clamping based on the traditional 3D CTA model is feasible in LPN.[5,6] However, this CTA model is characterized by limitations (ie, imprecise information on target arteries), leading to insufficient clamping and conversion to main renal artery clamping. A single vasculature model may be unable to determine the actual perfusion status of the renal parenchyma and tumor in a specific patient. In addition, the boundary of the resection is approximately 0.5 cm to the tumor capsule. The conventional CTA model may overlook/underestimate small branches feeding the surrounding normal parenchyma, leading to unexpected arterial bleeding from the parenchymal defect.

Fluorescence imaging using indocyanine green has been applied in the detection of target arteries during LPN.[19] Indocyanine green is injected following the selective clamping of segmental arteries, and the ischemic region determines the precision and effectiveness of the segmental artery clamping.[20-22] However, this method is unable to provide information on the vasculature of the renal hilum preoperatively. Inappropriate clamping of arteries during surgery may pose challenges to the adjustment of clamping, to meet the requirement of the ischemic region. Therefore, a novel model is required to precisely recognize the target arteries based on the parenchymal perfusion.

LPN with precise segmental artery clamping protects postoperative renal function. The GFR is an important index for the evaluation of renal function. The calculation of GFR includes the use of radionuclide renography and levels of SCr. However, radionuclide renography is costly, with potential radiation risk for patients. eGFR based on the levels of SCr is unable to provide information regarding split renal function and evaluate the affected renal function postoperatively. Recent studies have verified the feasibility of a new method to calculate GFR based on CT.[8] In this study, we calculated split (s) CT-GFR of both kidneys based on the 2-point Patlak plot technique through CTA. The results demonstrate a strong correlation between the split CT-GFR of the affected kidney and Ri-GFR ($R = 0.88$, $P < 0.01$).

Moreover, total (t)CT-GFR in the absence of a tumor had a stronger correlation with eGFR than tCT-GFR in the presence of a tumor. The 2-compartment model using the 2-point Patlak plot technique hypothesizes that the contrast agent is present in either the renal vessels or

Table 1. Patient characteristics and perioperative outcomes

Variables	
Patients, no.	91
Age, y, mean ± SD	56.5 ± 13.6
Male no. (%)	58 (63.7)
BMI, kg/m^2, mean ± SD	25.1 ± 3.1
RENAL nephrometry score, median (range)	5 (4-9)
Tumor size, cm, mean ± SD	2.9 ± 0.8
Growth pattern, no. (%)	
Exophytic	40 (44.0)
Mesophytic	36 (39.6)
Endophytic	15 (16.4)
Feeding lobar artery number, no. (%)	
1	15 (16.5)
2	41 (45.0)
3	28 (30.8)
4	6 (6.6)
5	1 (1.1)
Target segmental artery number, no. (%)	
1	56 (61.5)
2	32 (35.2)
3	3 (3.3)
Operative time, min, mean ± SD	81.8 ± 10.8
Warm ischemia time, min, mean ± SD	19.6 ± 3.6
EBL, mL, median (range)	120 (50-400)
Length of stay after operation, median (range)	6 (4-12)
eGFR, mL.min^{-1}.1.73m^{-2}, mean ± SD	96.5 ± 14.5
Postoperative complication, no.	
Grade 1 (hematuria not requiring intervention)	3
Grade 3a (postoperative bleeding requiring selective embolization intervention)	1
Pathology, no. (%)	
Clear cell carcinoma	76 (83.5%)
Perivascular epithelioid cell tumor	5 (5.5%)
Papillary renal cell carcinoma	4 (4.4%)
Chromophobe renal cell carcinoma	3 (3.3%)
Oxyphilic adenoma	2 (2.2%)
Liomyoma	1 (1.1%)

BMI, body mass index; EBL, estimated blood loss; eGFR, estimated glomerular filtration rate; SD, standard deviation.

kidney tubules. However, there is no normal and functional renal tissue inside the tumor. This part of the tumor tissue does not meet the criteria of the 2-compartment model. Therefore, the calculation of CT-GFR in the absence of a tumor is more suitable for the 2-compartment model, showing stronger correlation with eGFR.

CTA using DSCT has a section thickness of 0.75 mm and section increment of 0.5 mm. The scan provides clear imaging of segmental, lobar, and part of the interlobar arteries. Based on the spatial course of lobar arteries and anatomic theory, we depicted the perfusion demarcation of each segment. The results demonstrate consistency between the intraoperative ischemia boundary and the preoperative prediction by the novel perfusion model (Figs. 1, 2). The elemental measurable perfusion area is depicted based on lobar arteries, which are more distal and close to renal cortex than segmental arteries. However, most lobar arteries distribute within the parenchyma, the accessible target arteries are segmental rather than lobar arteries. The specific parenchymal area fed by segmental arteries may be depicted according to their bifurcated lobar arteries. Therefore, it is rational that the ischemic area in the parenchyma is invariably extended beyond the tumor. Larger tumors are accompanied by more feeding lobar arteries. These lobar arteries may bifurcate from single or multiple segmental arteries. Thus, the association between tumor size and the number of segmental arteries remains undefined (Tables 2). Most patients (61.5%) had a single feeding segmental artery, whereas 83.5% of patients had multiple (2 or more) feeding lobar arteries. Hence, lobar arteries may be more valuable than segmental arteries in indicating tumor perfusion. For renal tumors supplied by 2 or more lobar arteries, this perfusion model provides more precise and visualized information than conventional CTA and avoids insufficient clamping as far as possible. In this study, the median estimated blood loss was 120 mL and there was no occurrence of arterial hemorrhage during resection.

The main advantage of this integrated model is that a single examination meets multiple requirements. First, it demonstrates renal vasculature similarly to conventional CTA, serving surgical orientation. Second, it marks

Table 2. The correlation of target artery number with tumor growth pattern and tumor size

Variable	Patients, No.	Growth Pattern, No. (%)			*P* value	Tumor Size, cm, mean± SD	*P* value
		Exophytic	Mesophytic	Endophytic			
Segmental artery, no.							
1	56	29 (51.8)	19 (33.9)	8 (14.3)	$P > 0.05$	2.9 ± 0.8	$P > 0.05$
2-3	35	11 (31.4)	17 (48.6)	7 (20.0)		3.0 ± 0.7	
Lobar artery, no.							
1	15	8 (53.3)	5 (33.3)	2 (13.3)	$P > 0.05$	2.1 ± 0.6	**$P < 0.05$**[*]
2	41	21 (51.2)	16 (39.0)	4 (9.8)		2.8 ± 0.7	
3-5	35	11 (31.4)	15 (42.9)	9 (25.7)		3.4 ± 0.5	**$P < 0.05$**[†]

SD, standard deviation.
[*] $P = 0.003$, the size of tumors fed by 1 lobar artery is significantly smaller than that of tumors fed by 2 lobar arteries.
[†] $P = 0.0001$, the size of tumors fed by 3 or more lobar arteries is significantly larger than that of tumors fed by 2 lobar arteries.

perfusion of the parenchymal area by different segmental arteries, more comprehensively and intuitively than conventional CTA, to determine the optimal clamping strategy. Third, it provides a reliable calculation of split renal function for the estimation of warm ischemia injury during nephron-sparing surgery. By comparing the basal and dynamic changes of renal function prior to and after the operation, this model may become an important follow-up examination. Based on this integrated functional model, renal parenchyma is divided into several segments by segmental arteries. Evaluation of each segmental function may be feasible, rendering the prediction of postoperative renal function possible.

CONCLUSION

The integrated 3D perfusion model is feasible in LPN with precise segmental artery clamping. This noninvasive model provides precise anatomic information based on the varied parenchymal perfusion of segmental arteries and a reliable calculation of split renal function.

Acknowledgments. We appreciated the tremendous work of Dr. Guanyu Yang and Dr. Lijun Tang. We declare that Dr. Shaobo Zhang, Dr. Guanyu Yang and Dr. Lijun Tang contributed equally in this work.

SUPPLEMENTARY MATERIALS

Supplementary material associated with this article can be found, in the online version, at https://doi.org/10.1016/j.urology.2018.12.023.

REFERENCES

1. Van Poppel H, Becker F, Cadeddu JA, et al. Treatment of localised renal cell carcinoma. *Eur Urol.* 2011;60:662–672.
2. Heuer R, Gill IS, Guazzoni G, et al. A critical analysis of the actual role of minimally invasive surgery and active surveillance for kidney cancer. *Eur Urol.* 2010;57:223–232.
3. Gill IS, Patil MB, Abreu AL, et al. Zero ischemia anatomical partial nephrectomy: a novel approach. *J Urol.* 2012;187:807–814.
4. Shao P, Qin C, Yin C, et al. Laparoscopic partial nephrectomy with segmental renal artery clamping: technique and clinical outcomes. *Eur Urol.* 2011;59:849–855.
5. Shao P, Tang L, Li P, et al. Precise segmental renal artery clamping under the guidance of dual-source computed tomography angiography during laparoscopic partial nephrectomy. *Eur Urol.* 2012;62:1001–1008.
6. Shao P, Tang L, Li P, et al. Application of a vasculature model and standardization of the renal hilar approach in laparoscopic partial nephrectomy for precise segmental artery clamping. *Eur Urol.* 2013;63:1072–1081.
7. Xu Y, Shao P, Zhu X, et al. Three-dimensional renal CT angiography for guiding segmental renal artery clamping during laparoscopic partial nephrectomy. *Clin Radiol.* 2013;68:e609–e616.
8. Kwon SH, Saad A, Herrmann SM, Textor SC, Lerman LO. Determination of single-kidney glomerular filtration rate in human subjects by using CT. *Radiology.* 2015;276:490–498.
9. Su C, Yan C, Guo Y, et al. Multi-detector row CT as a "one-stop" examination in the preoperative evaluation of the morphology and function of living renal donors: preliminary study. *Abdom Imaging.* 2011;36:86–90.
10. Kutikov A, Uzzo RG. The R.E.N.A.L. nephrometry score: a comprehensive standardized system for quantitating renal tumor size, location and depth. *J Urol.* 2009;182:844–853.
11. Finley DS, Lee DI, Eichel L, et al. Fibrin glue-oxidized cellulose sandwich for laparoscopic wedge resection of small renal lesions. *J Urol.* 2005;173:1477–1481.
12. Levey AS, Stevens LA, Schmid CH, et al. A new equation to estimate glomerular filtration rate. *Ann Intern Med.* 2009;150:604–612.
13. Patlak CS, Blasberg RG, Fenstermacher JD. Graphical evaluation of blood-to-brain transfer constants from multiple-time uptake data. *J Cereb Blood Flow Metab.* 1983;3:1–7.
14. Hackstein N, Wiegand C, Rau WS, Langheinrich AC. Glomerular filtration rate measured by using triphasic helical CT with a two-point Patlak plot technique. *Radiology.* 2004;230:221–226.
15. Dindo D, Demartines N, Clavien PA. Classification of surgical complications: a new proposal with evaluation in a cohort of 6336 patients and results of a survey. *Ann Surg.* 2004;240:205–213.
16. Martin 2nd RC, Brennan MF, Jaques DP. Quality of complication reporting in the surgical literature. *Ann Surg.* 2002;235:803–813.
17. Porpiglia F, Fiori C, Bertolo R, et al. Long-term functional evaluation of the treated kidney in a prospective series of patients who underwent laparoscopic partial nephrectomy for small renal tumors. *Eur Urol.* 2012;62:130–135.
18. Volpe A, Blute ML, Ficarra V, et al. Renal ischemia and function after partial nephrectomy: a collaborative review of the literature. *Eur Urol.* 2015;68:61–74.
19. Lee HJ, Chen K, Molchanov R, Schwentner C, Sim ASP. Feasibility of utilizing near-infrared fluorescence imaging with indocyanine green for super-selective arterial clamping in pure laparoscopic partial nephrectomy. *Int J Urol.* 2018;25:382–383.
20. Harke N, Schoen G, Schiefelbein F, Heinrich E. Selective clamping under the usage of near-infrared fluorescence imaging with indocyanine green in robot-assisted partial nephrectomy: a single-surgeon matched-pair study. *World J Urol.* 2014;32:1259–1265.
21. Borofsky MS, Gill IS, Hemal AK, et al. Near-infrared fluorescence imaging to facilitate super-selective arterial clamping during zero-ischaemia robotic partial nephrectomy. *BJU Int.* 2013;111:604–610.
22. Bjurlin MA, Gan M, McClintock TR, et al. Near-infrared fluorescence imaging: emerging applications in robotic upper urinary tract surgery. *Eur Urol.* 2014;65:793–801.